



## PHYSICAL MODELS FOR SIMULATING SHIP STABILITY AND HYDROSTATIC MOTIONS

Shyh-Kuang Ueng

*Department of Computer Science and Engineering, National Taiwan Ocean University, Keelung, Taiwan, R.O.C,*  
skueng@mail.sju.edu.tw

Follow this and additional works at: <https://jmstt.ntou.edu.tw/journal>



Part of the [Engineering Commons](#)

### Recommended Citation

Ueng, Shyh-Kuang (2013) "PHYSICAL MODELS FOR SIMULATING SHIP STABILITY AND HYDROSTATIC MOTIONS,"  
*Journal of Marine Science and Technology*. Vol. 21: Iss. 6, Article 8.

DOI: 10.6119/JMST-012-1121-1

Available at: <https://jmstt.ntou.edu.tw/journal/vol21/iss6/8>

This Research Article is brought to you for free and open access by Journal of Marine Science and Technology. It has been accepted for inclusion in Journal of Marine Science and Technology by an authorized editor of Journal of Marine Science and Technology.

---

## PHYSICAL MODELS FOR SIMULATING SHIP STABILITY AND HYDROSTATIC MOTIONS

### Acknowledgements

This research is supported by NSC of Taiwan under the grant numbered as NSC 98-2221-E-019-025.

# PHYSICAL MODELS FOR SIMULATING SHIP STABILITY AND HYDROSTATIC MOTIONS

Shyh-Kuang Ueng

Key words: ship motion simulator, physical-based animation, ship stability simulation, physics engine.

## ABSTRACT

In this paper, efficient physics models are presented for simulating ship hydrostatic motions caused by sea waves, cargoes and flooding water. Based on the stability theory of ship, a ship is regarded as a floating body whose stability is indicated by its *gravity*, *buoyancy* and *meta* centers. These stability centers are influenced by cargoes, sea waves, flooding water and the ship mass. Variations of these stability centers create torques and forces which cause the ship to heave, pitch and roll. Because of the irregularity of the ship shape, analytical solutions of these stability centers do not exist. In this work, a finite volume approach is employed to overcome this problem. At first, we split the ship body into cells by using a regular grid and distribute the ship mass, cargoes and flooding water into these cells. Then numerical methods and physics laws of floating body are utilized to compute the coordinates of these centers. Subsequently, torques and forces are calculated and utilized to create ship motions.

## I. INTRODUCTION

Ships have been utilized for fishing, transportation, recreation and adventures for thousands of years. Learning the knowledge of ship-handling is essential to our daily lives. In modern maritime training courses, ship motion simulators are widely used to teach people how to operate ships under different sea conditions. To become an effective learning tool, a ship motion simulator must be equipped with a physics engine which can simulate the maneuverability of ship as real as possible under a severe time constraint [10]. Scientists have developed some mathematical models for computing ship motions [1, 9, 16]. However, realizing these models requires tremendous computational costs, and thus these model are too slow for building real-time ship motion simulators. In this

paper, we propose efficient physical models for simulating hydrostatic ship motions caused by sea waves, cargoes and flooding water. Our physical models are based on the stability theory of ship. We widen the scope of conventional ship motion simulation techniques by using the gravity, buoyancy and meta centers of the ship to estimate the stability of the ship and compute the forces and torques acting on the ship so that the ship motions can be simulated in real time.

Since the ship shape is irregular, it is impossible to compute the stability centers analytically. To overcome this problem, we split the ship body into cells and distribute the ship mass, cargoes and flooding water into the cells. Thus, the stability centers, forces and torques can be computed by using finite volume methods. Furthermore three distinct coordinate systems are employed in the proposed models to specify the position and orientation of ship, the geometry of ship body, the external forces and ship motions so that the formulations of forces and ship motions are simplified and all essential entities can be efficiently calculated by using fundamental physical laws. The proposed models are efficient, realistic and flexible. Users are allowed to compose various simulation scenarios by loading cargoes into the ship, generating severe sea waves and creating holes on the ship hull. The resulted ship motions will be automatically animated in real time with decent visual effects.

The rests of this paper are organized as follows: Related researches on ship motion simulation are presented in Section II. In Sections III-VI, the proposed physical models are systematically formulated. To establish the theoretical background, the stability theory of ship is introduced in Section III. Then the coordinate systems and the wave model employed in the proposed ship motion models are described in Section IV. The computational grid and the algorithms for computing the stability centers are presented in Section V. The procedures for calculating ship motions are formulated in Section VI. Experimental results are presented and discussed in Section VII. The conclusion of this paper is drawn in the last section.

## II. RELATED WORK

When floating on sea surface, a ship is surrounded by two types of fluids, the air and the sea water. The material properties of air and water are different, and the boundary between

the air and the sea water may fluctuate with time. Therefore ship motions are difficult to model. Furthermore, the ship shape, draft and displacement also affect the motions of the ship. These factors make the modeling of ship motion even harder. Currently, most numerical algorithms for computing ship motions are based on the *strip theory*, developed in [9, 16]. These algorithms calculate ship motions by solving highly nonlinear partial differential equations. Users may spend hours of CPU time just to obtain a set of solutions for one or two ship motions [1]. These traditional numerical procedures are too slow for constructing ship motion simulators.

Some researchers proposed simplified governing equations and boundary conditions to model ship motions. In [20], Zhang *et al.* developed mathematical models for simulating the motions of a ship sailing inside a harbor. In their method, the forces acting on the ship are estimated first. Then, simplified differential equations are derived to model the relations between the forces and the accelerations of ship motions. Subsequently, the differential equations are solved by using a Runge-Kutta method to compute the ship motions. Since their models focus on the ship's motions inside harbors, only the physical models for surge, sway and yaw are developed. Another simple ship motion model is reported in [4]. The authors use the sea wave model proposed in [7] to generate sea waves. At each time step, the height field of the sea surface under the ship body is computed. Then, the tangent plane of the sea surface is calculated and the ship is rotated such that its orientation is aligned with the tangent plane. Their method can simulate heave, pitch and roll of a ship. However, sea waves are the sole force of the ship motions. The ship will stop moving immediately as soon as sea waves come to rest. This phenomenon is in conflict with the behaviors of a real ship.

Other researchers propose statistical methods to predict ship motions. In [17], Kalman filters are utilized to estimate ship motions. Their models rely on many ship parameters to tune the governing equations. If these parameters are absent, the simulation cannot be performed. In [11], an improved method for computing ship motions is proposed. Their method requires less ship data. However, the accuracy of their model is still dependent on the availability of ship parameters. In ship motion simulations, the ship models are usually fabricated. Real ship parameters are hard to estimate. In [21], another statistical method is proposed to predict ship motions. In their method, the status and motions of the ship at some previous steps are recorded and converted into a tensor field. Then the eigenvalues and eigenvectors of the tensor field are computed. Finally, a minor component analysis is conducted to predict the ship motion at the next time step. Their method is useful for short-term ship motion prediction. For a long term ship motion simulation, the accuracy of their method may be decreased by accumulated numerical errors.

Recently, in the computer graphics society, several CFD algorithms have been proposed to model the interactions between fluids and floating bodies. In [6], Foster and Metaxas

use the Navier-Stokes equations to compute liquid motions. They compute the time varying fluid surface based on the *marked particles* approach. Once the velocity field and the pressure field have been calculated, the forces acting on the floating objects are estimated. Subsequently, the motions of the floating objects are calculated by using the Lagrange equations of motions. In [19], a numerical model is proposed to generate waves. Then the drag, lift and buoyancy forces acting on the floating bodies are computed and used to estimate the interactions between waves and the floating bodies. In [3], Carlson *et al.* present the *Rigid Fluid* method to compute the coupling between rigid bodies and fluids. They regard rigid bodies as fluids. Thus the motions of fluids and objects can be modeled by using the Navier-Stokes equations. However, the rigid body motion constraints are enforced in the governing equations such that rigid objects are not allowed to deform. In [8], Kim *et al.* apply the divergence theorem to convert volume integration into surface integration and use graphical hardware to speed up the computations. Then they utilize their hardware integration procedure to compute the gravity forces and buoyancy forces acting on floating bodies. In turn, the motions of floating objects are calculated by using these forces.

In [18], six mathematical models are proposed by Ueng *et al.* to simulate ship motions. In their method, the height field of the sea surface under the ship body is computed to estimate the external force acting on the ship. Then the external force is reduced by the damping effect of sea water to produce the net external force. The magnitudes of heave, pitch and roll are computed by using the net external force. They also proposed mathematical models to compute the gross internal force produced by the ship's propellers and rudders. Then the resistance of sea water is subtracted from the gross internal force to generate the net internal force. In the following step, the magnitudes of surge, sway and yaw are computed by using the net internal force. Finally, the six motions are super-imposed to generate the resulted ship motions. Their method allows users to tune ship motions according to the ship shape, draft and mass. Therefore ships of different shapes can behave differently under the same sea condition. The simulation results produced by using their models are physically sound and visually realistic.

However, all the aforementioned ship motion simulation methods are not based on the stability theory of ship. Ship motions caused by unbalanced cargo loading, body damages and severe sea conditions are not or only partially modeled. In their models, a ship can always retain its initial stability under any circumstances. It will not list, overturn and sink even it is loaded with heavy cargoes, encounters severe sea conditions or bears serious ship hull damages. Therefore, these models are in conflict with the real hydrostatic behaviors of ships. In this article, a new set of physical models are proposed to supplement these conventional ship motion models such that the hydrostatic behaviors of ships can be better simulated.

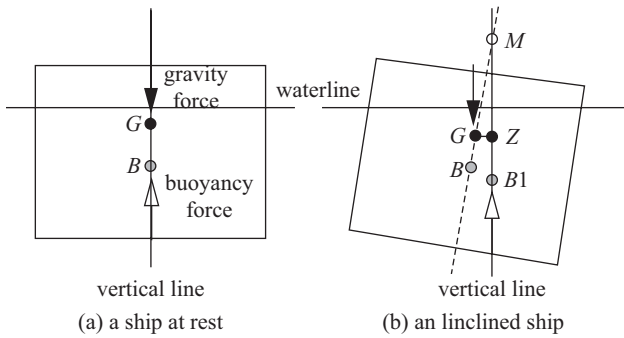


**Fig. 1. The gravity center  $G$ , buoyancy center  $B$  and meta center  $M$  of a ship. (a) When the ship rests on a flat water surface,  $G$  and  $B$  are collinear. (b) As the ship inclines,  $B1$  becomes the buoyancy center and  $M$  is located at the intersection of the line passing  $B$  and  $G$  and the vertical line passing  $B1$ .**

### III. THE STABILITY THEORY OF SHIP

Our physical models are based on the stability theory of ship. The fundamental knowledge of ship stability is briefly presented in this section. Detail description about this topic can be found in the books written by Lewis [12-14] and Derrett [5].

#### 1. The Stability Centers

The stability of a ship is decided by its gravity, buoyancy and meta centers [5]. The gravity center  $G$  is the point at which the mass of the ship is concentrated. The gravity force is considered to act downward at  $G$ . The magnitude of the gravity force is equal to the weight of the ship. The buoyancy center  $B$  is the geometrical center of the underwater portion of the ship. It is also the geometrical center of the displaced water body. The buoyancy force acts vertically upward at  $B$ . According to Archimedes principle, the magnitude of the buoyancy force is equal to the weight of the displaced water body.

When the ship floats at rest on flat sea surface, the gravity center and the buoyancy center are located at the same vertical line [5], as shown in the part (a) of Fig. 1. The magnitudes of the gravity force and the buoyancy force are equal, but these two forces act in opposite directions. If the magnitudes of these two forces are different, an external force is generated and the ship will heave upward or downward. If the ship inclines or the water surface varies, the buoyancy center will move to a new position  $B1$ , as depicted in the part (b) of Fig. 1. Since the gravity force and the buoyancy force no longer act in the same vertical line, a rotational torque is created and causes the ship to roll or pitch.

The vertical line passing the new buoyancy center  $B1$  will intersect the line passing  $B$  and  $G$ . The intersection point is called the meta center  $M$  of the ship. The meta center is the indication of stable equilibrium. If  $M$  is above  $G$ , the ship is in a stable equilibrium. The ship will retain its posture after making successive motions. On the other hand, if  $M$  is below

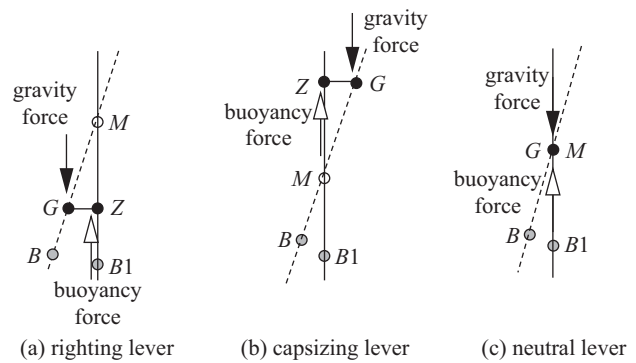


**Fig. 2. Three different levers created by the gravity and buoyancy forces, (a)  $G$  is under  $M$ , a righting lever, (b)  $G$  is above  $M$ , a capsizing lever, (c)  $G = M$ , a neutral lever.**

$G$ , the ship is in an unstable equilibrium. It will *capsize* to gain a new stability. On occasions,  $M$  coincides with  $G$  and the ship is in a neutral equilibrium. Any external force will change its posture forever.

#### 2. The Levers of Stability

These three equilibriums are illustrated in Fig. 2. Assume that the perpendicular projection of  $G$  in the vertical line passing through  $B1$  is  $Z$ . Then the edge  $GZ$  serves as a lever which creates a torque to change the posture of the ship. In the part (a),  $M$  is above  $G$  and the ship is in a stable equilibrium. The edge  $GZ$  is a righting lever which tends to bring the ship back to its original posture. In the part (b),  $M$  is below  $G$  and the ship is in an unstable equilibrium. The edge  $GZ$  is a capsizing lever which makes the ship rotate further until the ship obtains a new balance. A neutral equilibrium is shown in the part (c). In this case,  $G$  is coincident with  $M$ . Any force will change the posture of the ship.

### IV. THE COORDINATE SYSTEMS AND WAVE MODEL

In a ship motion simulation, many variables have to be updated at each time step, for examples, the orientation and position of the ship, the three stability centers, the forces and torques and the ship motions. Since the ship may vary its gesture and position constantly, specifying and computing all these variables in the world coordinate system will complicate the simulation. In the proposed physical models, three distinct coordinate systems are employed to define these entities such that essential computations are localized and simplified. Sea waves produce forces and vary the position, posture and orientation of the ship. Sea waves are an important cause of ship motions. The wave model used in our work is also presented in this section.

#### 1. The Coordinate Systems

The three coordinates systems used in the proposed physical models are shown in Fig. 3. The first coordinate system is

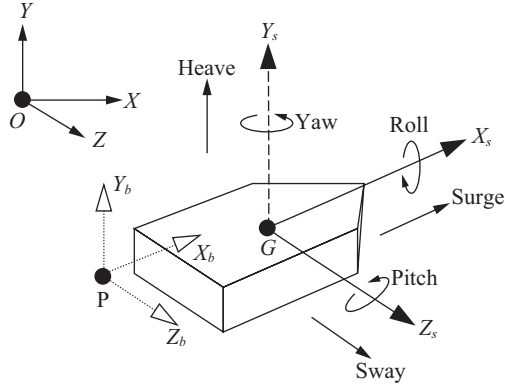


Fig. 3. Three coordinate systems and the six ship motions.

the world coordinate system which is used to designate the ship's position and orientation and model sea waves. In the world coordinate system, the sea surface is spanned by the  $X$  and  $Z$  axes. The  $Y$  axis is pointed vertically to the sky. The second coordinate system is the *body* coordinate system. This coordinate system is attached to the bounding box of the ship body and moved with the ship. The three axes,  $X_b$ ,  $Y_b$  and  $Z_b$ , are aligned with the bounding box boundaries. This coordinate system is used to define the geometrical mesh of the ship body and the positions of the three stability centers.

The third coordinate system is the *sea-keeping* coordinate system. It is used to specify and compute the forces and ship motions. Its origin is the gravity center  $G$ . The three axes of this coordinate systems are  $X_s$ ,  $Y_s$  and  $Z_s$ . The  $X_s$  axis is aligned with the forward direction of the ship. The  $Z_s$  axis is horizontally pointed to the starboard (right side) of the ship, and the  $Y_s$  axis is directed vertically upward. In this coordinate system, heave is the translate motion along the  $Y_s$  axis, pitch is the rotation about the  $Z_s$  axis, and roll is the rotation about the  $X_s$  axis. When the ship rests on a flat water surface, the axes of the body and sea-keeping coordinate systems are parallel, but the two origins are separated by a fixed distance. However, as the ship moves, the axes of these two coordinate systems will not coincide. For example, when the ship inclines, so does the bounding box. The  $X_b$  is rotated about the  $Z_s$  axis, but the axis  $X_s$  is not changed. The axis  $X_s$  always points to the forward direction of the ship and is parallel to the flat water surface.

## 2. The Wave Model

Sea waves are usually modeled as a time-dependent height field. A widely used sea wave model is proposed in the papers of [7, 15]. To increase the fidelity of sea waves, we assume that sea waves are composed of several sinusoidal waves of different frequencies, amplitudes, speeds and directions [18]. In our work, sea waves are defined by:

$$h(x, z, t) = \sum_{i=1}^n A_i \sin\left(\frac{2\pi}{\lambda_i} ((x \cos \theta_i - z \sin \theta_i) - \omega_i t)\right), \quad (1)$$

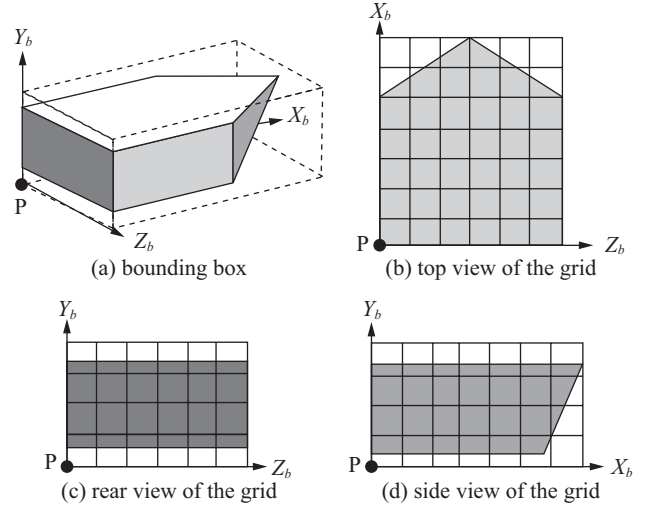


Fig. 4. The computational grid. (a) The bounding box, (b) top-view of the grid, (c) rear view of the grid, and (d) side view of the grid.

where  $A_i$ ,  $\lambda_i$  and  $\omega_i$  are the amplitude, wave length and speed of the  $i$ -th sinusoidal wave. The variable  $\theta_i$  is the angle between the  $X$  axis of the world coordinate system and the incoming direction of the  $i$ -th sinusoidal wave, and  $t$  is the time variable. We employ this wave model to generate sea waves, because it offers straight forward mechanisms for generating various sea waves. Our ship physical models are independent of this wave model. If it is necessary, this wave model can be replaced by other wave models.

## V. COMPUTING THE STABILITY CENTERS

The three stability centers affect the ship's stability. Variations of these stability centers generate forces and torques and trigger ship motions. In this section, the numerical methods for calculating the gravity centers are presented. Since the ship changes its posture and position frequently, specifying these centers in the world coordinate system is a difficult job. Thus they are computed in the body coordinate system.

### 1. The Computational Grid

Since the ship shape is irregular, the stability centers cannot be computed analytically. In this work, they are calculated by using a finite volume method. At first, the ship body is split into cells by using a regular grid, as shown in Fig. 4. The size of a cell is  $1\text{meter} \times 1\text{meter} \times 1\text{meter}$  ( $= 1$  cubic meter). The equivalent volume of water weighs about 1 ton. Then those cells which are outside the ship body are excluded. To do so, we associate each cell with a flag. If a cell is fully or partially contained in the ship body, its flag is set to 1. Otherwise its flag is set to 0 and this cell is excluded from the following computations. A cell with a flag value of 1 is called a *significant cell*.

Once the computational grid has been built, the ship mass, cargoes and flooding water are distributed to all the significant

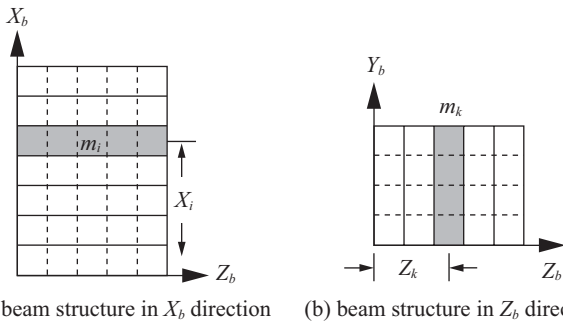


Fig. 5. The ship body is divided into cross-sections and treated as beam structures when computing  $G$ .

cells via a graphical user interface. In the ship motion simulation, users can add cargoes and flooding water into significant cells to alter the stability of the ship. Users can also remove the flooding water or cargoes from significant cells to reduce the mass of the ship.

2. Computing the Gravity Center  $G$

To compute the  $X_b$  coordinate of  $G$ , we group the significant cells with the same  $X_b$  coordinate into a slice and divide the ship body into  $L$  cross-sections in the  $X_b$  direction, as shown in the part (a) of Fig. 5. Then the ship body is treated as an 1-D beam structure. By applying the physical law for computing the gravity center of a beam, the  $X_b$  coordinate of  $G$  are calculated by:

$$X_b^G = (\sum_{i=1}^L m_i x_i) / M_s, \tag{2}$$

where  $X_b^G$  is the  $X_b$  coordinate of  $G$ ,  $m_i$  is the mass of the  $i$ -th cross-section,  $x_i$  is the  $X_b$  coordinate of the  $i$ -th cross-section center, and  $M_s$  is the ship mass. The value of  $m_i$  is calculated by summing up the masses of the significant cells of the  $i$ -th cross-section. The same approach is adopted to compute the  $Z_b$  coordinate of  $G$ . In this circumstance, the ship is divided into cross-sections along the  $Z_b$  axis, as shown in the part (b) of Fig. 5. The  $Y_b$  coordinate of  $G$  is calculated by following this procedure too.

3. Computing the Buoyancy Center  $B$

The buoyancy center  $B$  is the geometrical center of the immersed portion of the ship body. If the immersed portion has been figured out, the algorithm for computing  $G$  can be used to calculate the body coordinates of  $B$ .

To estimate the immersed portion, the grid of the ship body is vertically projected onto the  $X$ - $Z$  plane of the world coordinate system to create a 2D grid. Assume that the ship is not present, the wave model defined in Eq. (1) is employed to generate a height field in the 2D grid. Then the ship is brought back. The immersed portion of each significant cell is computed by comparing the sea surface height with the

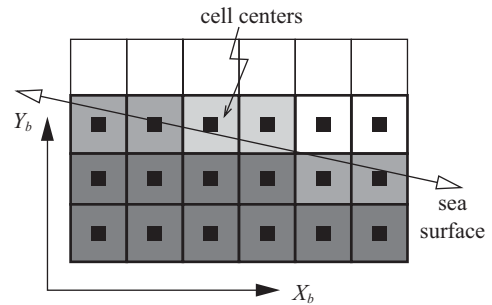


Fig. 6. The immersed portion of a cell is decided by the height of sea surface and the position of the cell center. The immersed volume of the ship body is equal to the sum of the immersed portions of the cells.

vertical position of the cell center. If the cell center is lower than the sea surface by more than one half of the cell width, the cell is totally immersed. If the cell center is higher than the sea surface by more than one half of the cell width, the cell is entirely above the sea surface and its immersed volume is zero. Otherwise, the volume of the immersed portion of the cell is computed by:

$$v_{im} = ((H_{sea} - C_y) / C_w) + 0.5 v_c, \tag{3}$$

where  $v_{im}$  is the immersed volume of the cell,  $H_{sea}$  is the height of the sea surface computed by using Eq. (1),  $C_y$  is the vertical position of the cell center,  $C_w$  is the width of the cell, and  $v_c$  is the volume of the cell.

The method of computing the immersed volume of the ship body is illustrated in Fig. 6. The ship are divided into cells. The cells shaded with the dark gray color are totally immersed while the cells shaded with light gray colors are partially immersed.

Once the immersed volumes of all significant cells have been calculated, the ship body is divided into  $L$  cross-sections in the  $X_b$  direction. The  $X_b$  coordinate of  $B$  is computed by:

$$X_b^B = (\sum_{i=1}^L \rho V_i x_i) / M_s, \tag{4}$$

where  $X_b^B$  is the  $X_b$  coordinate of  $B$ ,  $\rho$  is the density of sea water, and  $V_i$  is the volume of the immersed portion of the  $i$ -th cross-section.  $V_i$  is computed by summing up the immersed portions of the significant cells of the  $i$ -th cross-section. The other two body coordinates of  $B$  are computed by using this method too.

4. Computing the Meta Centers

The meta centers of pitch and roll are at different positions. Let's denote the two meta centers as  $M_p$  and  $M_r$ . According to the stability theory of ship [5], the vertical distances between  $B$  and the two meta centers can be analytically calculated by:

$$BM_p = (\text{breadth} * \text{length}^3) / (12M_s), \quad (5)$$

$$BM_r = (\text{length} * \text{breadth}^3) / (12M_s), \quad (6)$$

where *breadth* and *length* are the width and length of the ship body, and  $BM_p$  and  $BM_r$  are the vertical distances between  $B$  and the meta centers of pitch and roll. Since the meta centers are always vertically above  $B$ , their positions can be computed once  $B$ ,  $BM_p$  and  $BM_r$  are available.

## VI. PHYSICAL MODELS OF SHIP MOTIONS

As floating on the sea surface, a ship possesses six degrees of freedom, which include heave, pitch, roll, surge, sway and yaw, as shown in Fig. 3. These motions can be divided into two groups. The first group of motions are triggered by the ship's propellers, rudders, sea currents and winds. Surge, sway and yaw belong to this group. Through these motions, the ship navigates from one place to another. The other group of motions are induced by cargoes, flooding water inside the ship and sea waves. This motion group includes heave, pitch and roll. These motions vary the ship's posture and cause the ship to oscillate, capsize and sink. Thus the hydrostatic properties of the ship under different sea conditions are revealed. This paper mainly focuses on the development of physical models for animating the hydrostatic behaviors of ships. Therefore, only the physical models of heave, pitch and roll are considered. The physical models of other ship motions can be found in the paper of [18].

### 1. The Physical Model of Heave

The difference of the gravity force magnitude and the buoyancy force magnitude causes the ship to heave. As the ship heaves, the viscosity of sea water produces a resistance force to keep the ship from moving upward and downward. Assume that the resistance force is related to the moment of heave and the ship shape. The net force for heave is estimated by:

$$R_h = b_h M_s \bar{v}_h, \quad (7)$$

$$F_h = (W_w - W_s) - R_h. \quad (8)$$

In Eq. (7),  $R_h$  is the resistance force,  $b_h$  is the damping coefficient of heave,  $M_s$  is the ship mass, and  $\bar{v}_h$  is the current heave velocity. In Eq. (8),  $F_h$  is the net force for heave,  $W_w$  is the weight of the displaced water body and is equal to the buoyancy force, and  $W_s$  is the ship weight which is equal to the gravity force. The net force  $F_h$  is obtained by subtracting the resistance force  $R_h$  from the *surplus* of the buoyancy force  $W_w$  over the gravity force  $W_s$ . Once the net force has been obtained, the acceleration and velocity of heave are computed and updated by:

$$a_h = F_h / M_s, \quad (9)$$

$$\bar{v}_h = \bar{v}_h + a_h \Delta t, \quad (10)$$

where  $a_h$  is the acceleration of heave and  $\Delta t$  is the time step size. Finally, the magnitude of heave is calculated by:

$$\Delta \text{heave} = \bar{v}_h \Delta t, \quad (11)$$

$$\text{heave} = \text{heave} + \Delta \text{heave}. \quad (12)$$

### 2. The Physical Model of Pitch

If the gravity center and the buoyancy center are not col-linear, the buoyancy force exerts a rotational torque and forces the ship to pitch and roll, as shown in the parts (a) and (b) of Fig. 2. Let  $Z$  be the perpendicular projection of the gravity center  $G$  in the vertical line passing the buoyancy center  $B1$ , as shown in the parts (a) and (b) of Fig. 2. The edge  $GZ$  acts as the lever of rotation. By calculating the moments at  $G$ , the magnitude of the rotational torque is defined as:

$$\tau = W_w * \|GZ\|, \quad (13)$$

where  $W_w$  denotes the weight of the displaced water body and  $\|GZ\|$  is the length of the lever.

In the sea-keeping coordinate system, pitch is the rotation about the  $Z_s$  axis and triggered by the  $X_s$  component of the rotational torque. Thus, the force of pitch is equal to the  $X_s$  component of the rotational torque. As the ship pitches, the resistance of sea water will prevent the ship from inclining or tilting further. Assume that the resistance force is proportional to the speed of pitch but exerts in the opposite direction. Then the magnitude of the net force of pitch is determined as follows:

$$\tau_p = W_w * \langle GZ, \bar{X}_s \rangle, \quad (14)$$

$$F_p = \tau_p - b_p I_p \omega_p. \quad (15)$$

In Eq. (14),  $\tau_p$  is the magnitude of the torque of pitch,  $\langle \rangle$  is the inner-product operator,  $\bar{X}_s$  is the directional vector of the  $X_s$  axis, and  $GZ$  is the vector from  $G$  to  $Z$ . In Eq. (15), the magnitude of the net force of pitch,  $F_p$ , is obtained by subtracting the resistance from the magnitude of the torque of pitch. The resistance is determined by the damping coefficient  $b_p$ , the inertia of moment  $I_p$  and the current pitch speed  $\omega_p$ .

Then the magnitudes of acceleration, speed and angle of pitch are computed by:

$$\alpha_p = F_p / I_p, \quad (16)$$

$$\omega_p = \omega_p + \alpha_p \Delta t, \quad (17)$$



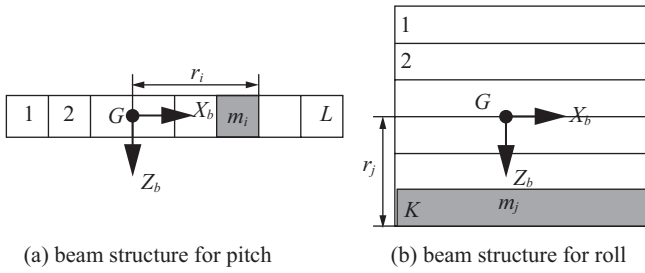


Fig. 7. Beam structures for computing the inertia moments. (a) For computing the inertia moment of pitch, the ship body is divided into cross-sections along the  $X_b$  axis. (b) The ship body is divided into cross-sections along the  $Z_b$  axis for computing the inertia moment of roll.

$$\Delta\theta_p = \omega_p \Delta t, \tag{18}$$

$$\theta_p = \theta_p + \Delta\theta_p, \tag{19}$$

where  $\alpha_p$  is the angular acceleration magnitude of pitch and  $\theta_p$  is the angle of pitch.

The inertia moment  $I_p$  in computing pitch plays the same role as the ship mass in calculating heave [2]. To compute  $I_p$ , the ship is divided into  $L$  cross-sections and regarded as a beam, as shown in the part (a) of Fig. 7. Based on physical laws, the inertia moment  $I_p$  is calculated by:

$$I_p = \sum_{i=1}^L m_i r_i^2, \tag{20}$$

where  $r_i$  is the difference of the  $X_b$  coordinates of  $G$  and the  $i$ -th cross-section center and  $m_i$  is the mass of the  $i$ -th cross-section.

### 3. The Physical of Roll

The physical model of roll is similar to that of pitch. To compute the angle of roll, the  $Z_s$  component of the rotational torque is computed first. Then the magnitude of the net force of roll is obtained by subtracting the resistance of sea water from the magnitude of torque of roll:

$$\tau_r = W_w^* \langle GZ, \vec{Z}_s \rangle, \tag{21}$$

$$F_r = \tau_r - b_r I_r \omega_r, \tag{22}$$

where  $\tau_r$  and  $F_r$  are the magnitudes of the torque and the net force of roll, and  $b_r$ ,  $I_r$  and  $\omega_r$  are the damping coefficient, inertia moment and speed of roll.

In turn, the net force magnitude is used to compute the acceleration magnitude of roll  $\alpha_r$ . The speed of roll  $\omega_r$  is updated once the acceleration magnitude is available. The increment of roll angle is decided by multiplying the roll speed with the time step size:

$$\alpha_r = F_r / I_r, \tag{23}$$

$$\omega_r = \omega_r + \alpha_r \Delta t, \tag{24}$$

$$\Delta\theta_r = \omega_r \Delta t, \tag{25}$$

$$\theta_r = \theta_r + \Delta\theta_r, \tag{26}$$

where the angle of roll is represented by  $\theta_r$ .

To estimate  $I_r$ , the ship is treated as a beam with  $K$  cross-sections as shown in the part (b) of Fig. 7. By using the same method for computing the inertia moment of pitch,  $I_r$  is approximated by:

$$I_r = \sum_{j=1}^K m_j r_j^2, \tag{27}$$

where  $m_j$  is the mass of the  $j$ -th cross-section, and  $r_j$  is the difference of the  $Z_b$  coordinates of  $G$  and the  $j$ -th cross-section center.

### 4. The Damping Coefficients

The damping coefficients  $b_n$ ,  $b_p$  and  $b_r$  are critical parameters in our physical models. They decide the converge rates and magnitudes of the ship motions. Smaller damping coefficients result in longer and larger oscillations, while larger damping coefficients produce shorter and smaller oscillations. In our models, these coefficients are confined to the range of  $\{0 \sim 2\}$ , but users are allowed to modify these coefficients to enhance or reduce the magnitudes and durations of ship motions. Some default values of these coefficients are predefined in our physical models for special types of ship. For example, the damping coefficients of a massive and streamlined war ship are set to 1.3. Therefore, the war ship is relatively insensitive to sea waves. On the other hand, these coefficients of a raft are set to 0.5 so that the raft can fluctuate with sea waves.

## VII. EXPERIMENTAL RESULTS AND ANALYSIS

Based on our physical models, a ship motion simulator is created to animate hydrostatic behaviors of ships. The embedded computer of our simulator is a desk-top machine equipped with an Intel Core2 CPU of 1.86 GHz clock rate and an Nvidia GeForce 8800 GTS GPU. The rendering subroutine is implemented by using OpenGL libraries. The computational modules are designed by using C-language. Some basic and compound ship motions are simulated by using our system. The results are presented and discussed in this section.

The main Graphical User Interface (GUI) of the system is shown in the part (a) of Fig. 8. The main GUI composes of the main screen which shows the motions of the ship and a sub-window which displays the path of the ship. The other two key GUI are depicted in the parts (b) and (c). In the part

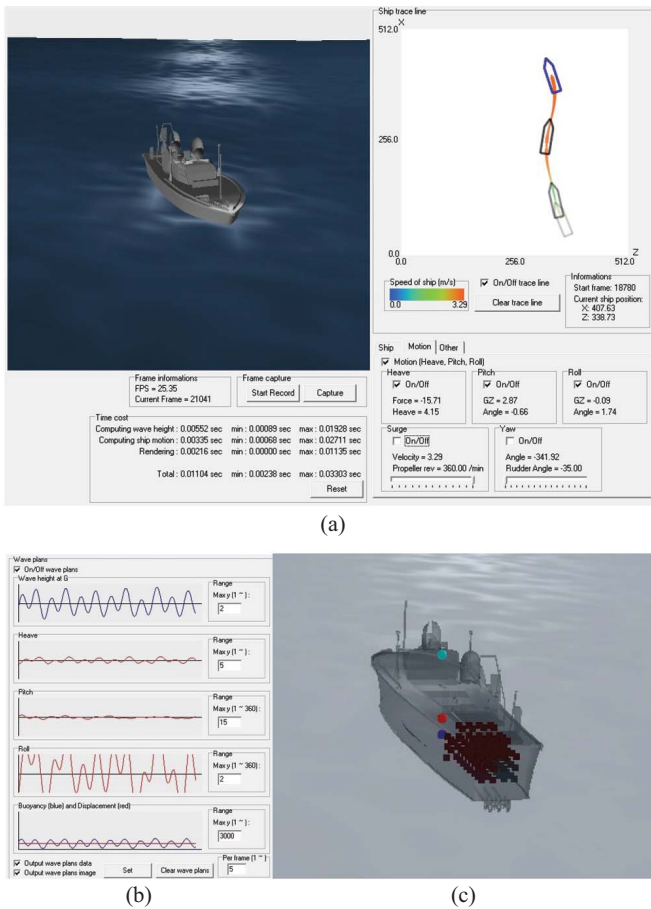


Fig. 8. (a) The main GUI of the simulator, (b) the window to the show wave height and motion magnitudes, (c) the GUI to load and unload cargoes and create body damage.

(b), the wave height under the gravity center and the magnitudes of motions of the elapsed time steps are shown so that the effects of waves on the stability of the ship can be revealed. In the part (c), the GUI in which users load or unload cargoes and water into the significant cells is illustrated. In our implementation, only some significant cells are allowed to store cargoes and water. These cells are shown by gray cubes in this image. The stability centers are also displayed to demonstrate the influence of the loadings toward the stability of the ship.

### 1. Basic Motions: Heave and Pitch

In the first experiment, a simple ship model is loaded into our simulator to perform heave and pitch motions. Four images of the heave motion simulation are shown in the parts (a)-(d) of Fig. 9. In these images, the gravity center  $G$  and the buoyancy center  $B$  are represented by a red ball and a blue ball respectively. The ship body and sea water are rendered as transparent objects such that the variations of  $G$  and  $B$  can be monitored.

Initially, we exert an external force on the ship and press the ship downward, as shown in the part (a). Since the

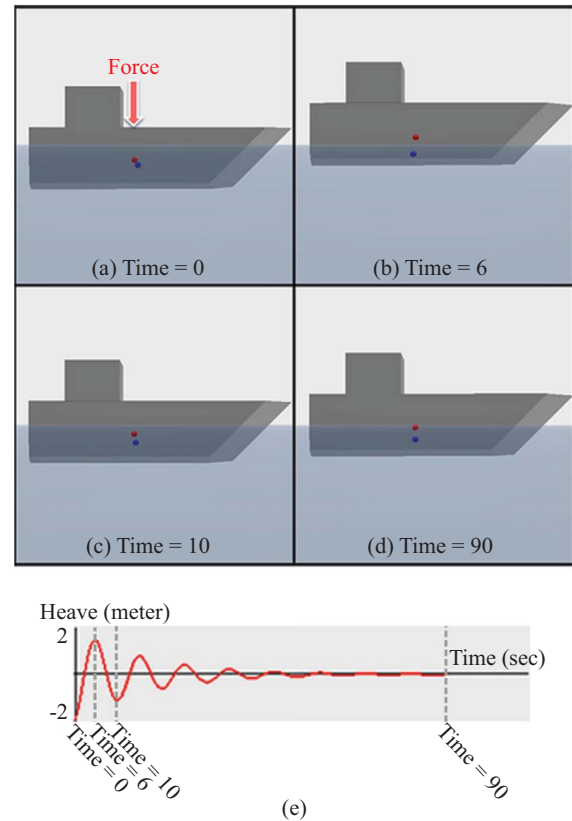


Fig. 9. (a)-(d) Snapshots of the heave motion of a ship, (e) the magnitude of the heave motion at each time step.

immersed portion of the ship is increased, the buoyancy force magnitude is larger than the gravity force magnitude. When the external force is released, the buoyancy force lifts the ship upward immediately, as illustrated in the part (b). As the ship moves upward, the buoyancy force magnitude is decreased. The resistance of sea water and the gravity force gradually reduce the heave velocity to zero. At this moment, the ship starts to fall because of the gravity force. The result is displayed in the part (c). As the ship falls, the buoyancy force magnitude is increased again and becomes greater than the gravity force magnitude. Thus the ship is pushed upward again. After a series of oscillations, the resistance of sea water wears down the force of heave. Finally, the ship retains its balance, as shown in the part (d). The magnitude of the heave motion at each time step is shown in the part (e). As shown by the graph, the heave magnitude oscillates and gradually converges to zero as time elapses.

Another four images are displayed in Fig. 10 to illustrate the pitch motion of the ship. Initially, a force is exerted on the ship's front end. The force causes the ship to incline forward as shown in the part (a). Since the gravity center and the buoyancy center are not collinear, a rotational torque is created. As the force is released, the rotational torque makes the ship tilt upward, as shown in the part (b). Then the damping force of sea water cancels the rotational torque and

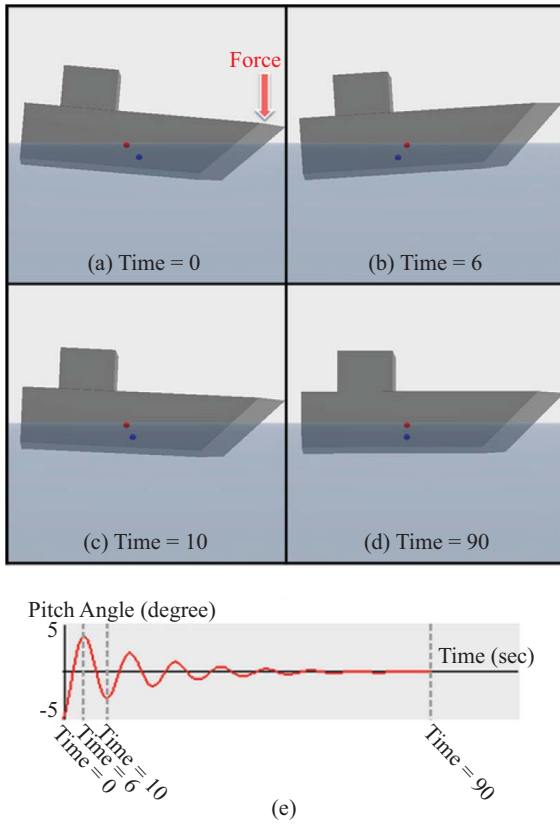


Fig. 10. (a)-(d) Snapshots of the pitch motion of a ship, (e) the magnitude of the pitch motion at each time step.

prevents the ship from tilting upward further. However,  $G$  and  $B$  are not collinear either at this moment. The gravity force creates another rotational torque to incline the ship, as displayed in the part (c) of this figure. Finally, after pitching back and forth for several rounds, the damping effects of sea water diminish the rotational torque and the ship recovers its stability, as illustrated in the part (d).

The variations of the pitch angle are depicted in the part (e). Initially, the external force causes the ship to pitch by 5 degrees. Then the gravity force and the buoyancy force make the pitch angle fluctuate periodically. As time elapses, the damping effects of sea water reduce the rotational torque to zero, and the pitch motion gradually converges to rest. This graph shows a typical behavior of a inclined floating body. It verifies the validity of our pitch model.

**2. Compound Motion: Wave Induced Motions**

When encountering sea waves, a ship will heave, pitch and roll simultaneously. The resulted motions are called *wave-induced motions* in sea-keeping literatures. In another experiment, the motions of a speed boat encountering sea waves are simulated by using our simulator. Some results are presented and analyzed in this section. The fundamental data of the speed boat are listed in Table 1. The ship weighs about 523 tons. Its length is about 40 meters. In order to enhance

**Table 1. Geometrical and damping coefficients of the speed boat.**

Geometrical coef.	Length = 40 m	Width = 10 m	Height = 15 m
	Weight = 523 t	Draft = 5.05 m	
Damping coef.	$b_h = 1.6$	$b_p = 0.6$	$b_r = 0.4$

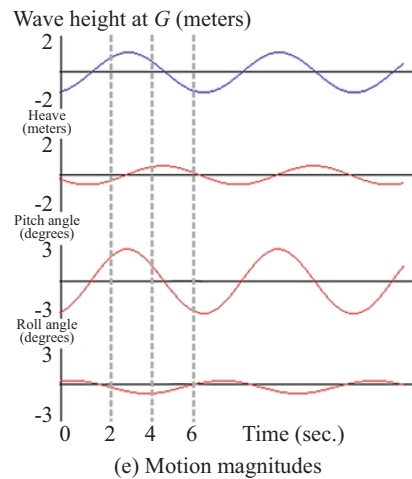
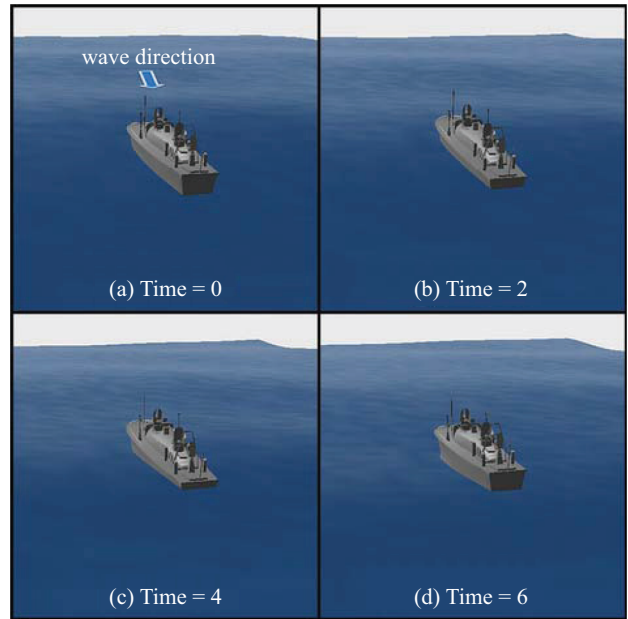


Fig. 11. (a)-(d) Snapshots of the wave-induced motions, (e) the wave height at  $G$  and the magnitudes motion at each time step.

the visual effects of the simulation, the damping coefficients of pitch and roll are set to 0.6 and 0.4. Therefore, the motions are exaggerated and last longer. The sea waves are composed of three sinusoidal waves of different frequencies, directions and amplitudes. The major sea wave approaches the ship from the north-east direction.

Four snapshots of the simulation are shown in Fig. 11. The initial scene is displayed in the part (a). At this moment, the ship head is in a trough and a crest just passes the rear end.

**Table 2. Computational cost profiles of two ship motions (by seconds).**

	Wave-induced motion	sinking
Wave generation	0.00838	0.00838
Rendering	0.00258	0.00258
Motion computation	0.00161	0.00180
Frame rate	66 fps	64 fps

The ship heaves slightly downward and inclines forward because of the passing crest. Two time steps later, another crest reaches the front end and the ship starts to tilt upward. Since the water level under the ship body is still low and the buoyancy force magnitude is too small, the ship does not heave upward. The snapshot is presented in the part (b). As the new crest passing the ship body, the buoyancy force and the gravity force disturb the stability of the ship. The ship heaves, pitches and rolls simultaneously, as shown in the part (c). When this crest passes the rear end, the ship inclines forward. The ship's posture is displayed in the part (d).

In the part (e), the height of the sea level at the gravity center and the magnitudes of heave, pitch and roll at each time step are displayed. By examining these graphs, we can conclude that the variations of the sea waves indeed induce the motions. As the sea surface varies periodically, so do the motion magnitudes. However, there exist latencies between the variation of wave height and the ship motions, as shown in the 1st, 2nd and 4th graphs. These latencies are typical phenomena of wave induced motions and have been mentioned in the literature of [12]. Our physical models are able to produce these latencies in the experiment.

The profile of the computational costs of a frame is depicted in the 2nd column of Table 2. The costs of computing the sea waves and rendering the scene are contained in the 2nd and 3rd rows. The costs of computing the ship motions are listed in the 4th row. The frame rate of this simulation is recorded in the last row. Our system needs only about 0.00161 second to compute the ship motions. The rendering process consumes about 0.00258 second. (The ship model is composed of 7,000 polygons, and the sea surface contains 32,768 triangles.) The costs for computing the sea waves are about 0.00838 second. Since the sea waves are composed of three sinusoidal waves and the range of the sea surface is large, computing the sea waves requires more efforts than computing the ship motions. In total, the frame rate of the simulation is about 66 fps.

### 3. Compound Motion: Cargo Induced Motions

If a ship is loaded with unbalanced cargoes, its gravity center may be higher than its meta center. The ship will *capsize* to reach a new stable posture. (In sea-keeping literatures, the term, *capsize*, does not mean overturning. Instead, this term is used to describe the process of obtaining a new stability.) In another simulation, a ship of 1,200 tons of displacement is

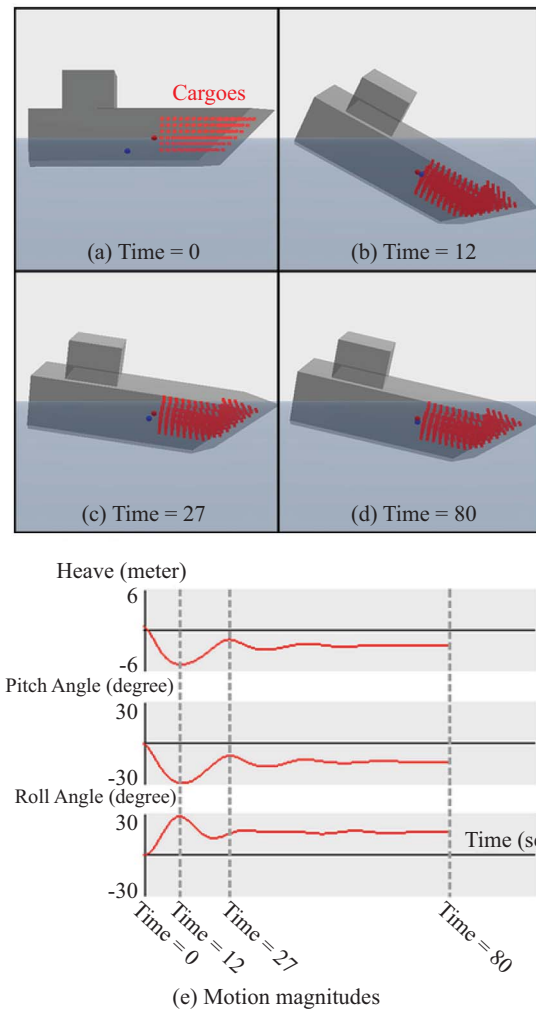


**Fig. 12. (a)-(d) Snapshots of the capsizing motions, (e) the wave height at  $G$  and the magnitudes of motion at each time step.**

served as the ship to simulate the ship motions caused by unbalanced cargoes. The damping coefficients of the ship are decreased to 0.1 such that the ship motions are exaggerated. Four images of the simulation are presented in Fig. 12.

Initially, some heavy cargoes are loaded into the right front part of the ship. These cargoes are represented by red cubes, as shown in the part (a) of this figure. Since the right front part of the ship gains extra masses, the gravity center  $G$  (the red ball) is shifted ahead. The ship inclines forward and rolls right. At time  $T = 12$ , the heavy cargoes cause the ship to pitch downward. The ship head is totally immersed into sea water, and the buoyancy force magnitude is greatly increased, as shown in the part (b). The buoyancy force creates a righting lever to bring the ship back from the inclination. However, the heavy cargoes prevent the ship from recovering its initial stability. Instead, the ship can only tilt back by a few degrees. The scenario is displayed in the part (c). At this moment, the ship head reaches its highest position. Then the gravity force causes the ship to incline forward and heave



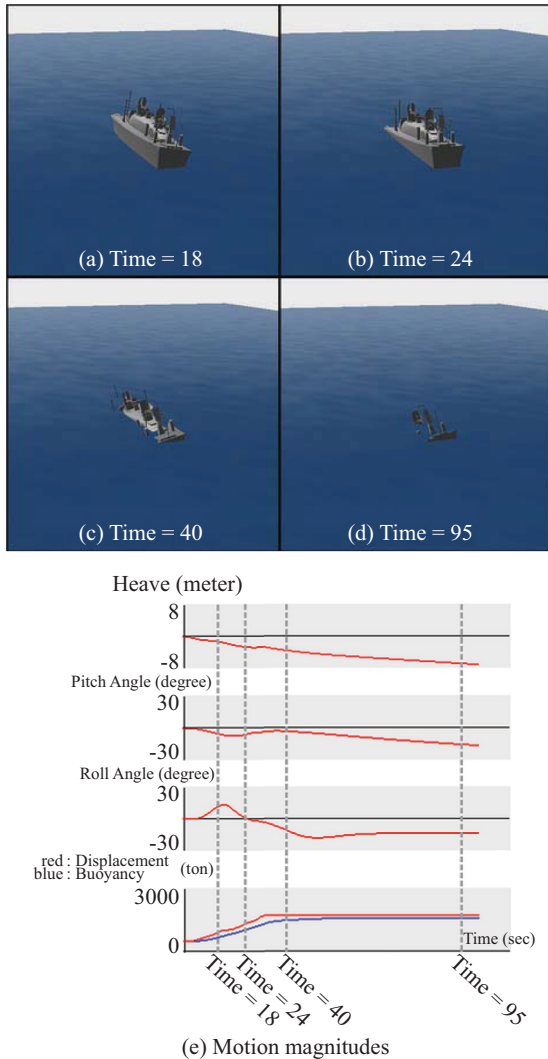


Fig. 13. (a)-(d) Snapshots of the sinking motions, (e) the wave height at  $G$  and the magnitudes of motion at each time step.

downward again. In this manner, the ship oscillates for several rounds. Then the motion magnitudes are gradually reduced by the damping effects of sea water, and the ship obtains a new stability at  $T = 80$ , as shown in the part (d).

The variations of the motion magnitudes are shown in the part (e). In this experiment, there is no sea wave. The only external force is created by the heavy cargoes. At  $T = 12$ , the ship heaves downward by about 6 meters and pitches forward and rolls right by about 30 degrees. The ship motion magnitudes reach their maxima at this time step. When reaching the new stability, the ship's position is lowered by 2 meters and inclined forward and rolled right by about 12 degrees.

**4. Sinking Caused by Flooding Water**

If a ship bears severe ship hull damages and too much water floods into the ship, the ship weight will exceed the weight of the maximum displaced water body. Thus the buoyancy force

cannot support the ship weight and the ship will sink. In the last simulation, we create holes in the right-front side of the speed boat and let sea water leak into its body. As sea water floods into the ship, the ship weight exceeds the maximum buoyancy force magnitude that the ship body can produce. Subsequently, the ship sinks into the sea.

Four snapshots of the sinking process are shown in Fig. 13. At  $T = 18$ , a small volume of sea water leaks into the boat. The boat pitches forward, rolls to the right and heaves downward, as shown in the part (a). As more water floods into the ship body, the ship stops rolling but its head is immersed into the sea. The result is displayed in the part (b). At  $T = 40$ , more cells of the ship body are occupied by sea water and the speed boat rolls to the left and heaves downward, as illustrated in the part (c). At  $T = 95$ , too much water has flooded into the ship, and thus most part of the ship sinks into the sea. The result is shown in the part (d).

In the part (e) of this figure, the motion magnitudes, the ship displacement and the buoyancy force magnitude at each time step are depicted. The heave magnitude at each time step is displayed in the first graph. The heave magnitude is always negative (downward). The ship displacement and the buoyancy force magnitude are represented by the red curve and the blue curve respectively in the last graph. Before  $T = 40$ , the displacement and the buoyancy force magnitude increase simultaneously. At  $T = 53$ , the displacement and the buoyancy force magnitude reach their maxima, but the displacement is larger. Therefore, the ship is doomed to sink.

The costs of the sinking simulation are described in the 3rd column of Table 2. It takes about 0.00180 second to compute the motions for each time step. As sea water flooding into the ship body, the ship gets extra weights. Our simulator has to re-calculate  $G$  in each frame. Therefore the costs for simulating the sinking process are slightly higher than those for simulating the wave-induced motions. The frame rate of this simulation is about 64 fps.

**VIII. CONCLUSION**

In this article, efficient methods for computing ship motions are presented. In our methods, we use the gravity, buoyancy and meta centers to predict the stability of the ship and compute the external forces causing ship motions. Based on our models, we implement a ship motion simulator to simulate various ship motions. Experimental results verify that our methods are physically sound and capable of simulating compound ship motions in real time with decent visual effects. In traditional ship motion models, sea waves are the sole factor which triggers ship motions. Our models cope with not only sea waves but also flooding water and cargoes. Users are allowed to compose complex ship motions by modifying the environment and the ship parameters. For examples, they can change the damping coefficients, add cargoes into the ship and create holes on the ship hull. Our ship motion simulator can generate the entire sequence of the ship motions auto-

matically in real time to reveal the hydrostatic behaviors of the ship. Beside computing the ship motions, our simulator also exhibits the variations of key parameters in ship motion simulations. By examining the output data, users can learn more knowledge about sea-keeping and hydrostatic properties of ships.

### ACKNOWLEDGMENTS

This research is supported by NSC of Taiwan under the grant numbered as NSC 98-2221-E-019-025.

### REFERENCES

1. Aryanpour, M. and Ghorashi, M., "Heave and pitch motions of a ship due to moving masses and forces," *Journal of Sound and Vibration*, Vol. 241, pp. 185-195 (2001).
2. Benson, H., *University Physics*, John Wiley & Sons, Inc. (1996).
3. Carlson, M., Mucha, P. J., and Turk, G., "Rigid fluid: Animating the interplay between rigid bodies and fluid," *ACM Transactions on Graphics*, Vol. 22, No. 3, pp. 377-384 (2004).
4. Cieutat, J. M., Gonzato, J. C., and Guitton, P., "A new efficient wave model for maritime training simulator," *IEEE Spring Conference on Computer Graphics*, pp. 202-209 (2001).
5. Derrett, D. R., *Ship Stability*, Butterworth-Heinemann (2000).
6. Foster, N. and Metaxas, D., "Realistic animation of liquids," *Graphical Models and Image Processing*, Vol. 58, No. 5, pp. 471-483 (1996).
7. Fournier, A. and Reeves, W. T., "A simple model of ocean waves," *Proceedings of SIGGRAPH'86*, pp. 75-84 (1986).
8. Kim, J., Kim, S., Ko, H., and Terzopoulos, D., "Fast gpu computation of the mass properties of a general shape and its application to buoyancy simulation," *Visual Computer*, Vol. 22, No. 9, pp. 856-864 (2006).
9. Korvin-Kroukovsky, B. V. and Jacobs, W. R., "Pitching and heaving motions of a ship in regular waves," *Transactions of the Society of Naval Architects and Marine Engineers*, pp. 590-632 (1957).
10. Kuhl, J., Evans, D., and Papelis, Y., "The Iowa Driving Simulator: an immersive research environment," *Computer*, Vol. 28, No. 7, pp. 35-41 (1995).
11. Lainiotis, D. G., Charalampous, C., Giannakopoulos, P., and Katsikas, S., "Real time ship motion estimation," *Proceedings of OCEAN'92 Conference*, pp. 283-287 (1992).
12. Lewis, E. V., *Principles of Naval Architecture, Volume I Stability and Strength*, Society of Naval Architects (1988).
13. Lewis, E. V., *Principles of Naval Architecture, Volume II Resistance, Propulsion, and Vibration*, Society of Naval Architects (1990).
14. Lewis, E. V., *Principles of Naval Architecture, Volume III Motions in Waves and Controllability*, Society of Naval Architects (1990).
15. Peachy, D., "Modeling waves and surf," *Proceedings of SIGGRAPH'86*, pp. 65-74 (1986).
16. Salvesen, N., Tuck, E. O., and Faltinsen, O., "Ship motions and sea loads," *Transactions of the Society of Naval Architects and Marine Engineers*, pp. 250-287 (1970).
17. Triantafyllou, M. S., Bodson, M., and Athans, M., "Real time estimation of ship motions using Kalman filtering techniques," *IEEE Journal of Oceanic Engineering*, Vol. 8, No. 1, pp. 9-20 (1983).
18. Ueng, S.-K., Lin, D., and Liu, C.-H., "A ship motion simulation system," *Virtual Reality*, Vol. 12, No. 1, pp. 65-76 (2008).
19. Yuksel, C., House, D. H., and Keyser, J., "Wave particles," *ACM Transactions on Graphics*, Vol. 26, No. 3, Article No. 99 (2007).
20. Zhang, X., Jin, Y., Yin, Y., and Li, Z., "Ship simulation using virtual reality technique," *Proceedings of ACM Siggraph International Conference on Virtual Reality Continuum and its Applications in Industry*, pp. 282-285 (2004).
21. Zhao, X., Xu, R., and Kwan, C., "Ship-motion prediction: algorithms and simulation results," *Proceedings of IEEE International Conference on Acoustics, Speech, and Signal Processing*, Vol. 5, pp. 125-128 (2004).